REVIEW
PHYSIOLOGY 34: 409–418, 2019. Published October 2, 2019; doi:10.1152/physiol.00010.2019

Lunge Feeding in Rorqual Whales

Robert E. Shadwick,[1] Jean Potvin,[2] and Jeremy A. Goldbogen[3]

[1]Department of Zoology, University of British Columbia, Vancouver, British Columbia, Canada; [2]Department of Physics, Saint Louis University, St. Louis, Missouri; and [3]Department of Biology, Hopkins Marine Station, Stanford University, Pacific Grove, California
shadwick@zoology.ubc.ca

The largest animals are baleen filter feeders that exploit large aggregations of small-bodied plankton. Although this feeding mechanism has evolved multiple times in marine vertebrates, rorqual whales exhibit a distinct lunge filter feeding mode that requires extreme physiological adaptations—most of which remain poorly understood. Here, we review the biomechanics of the lunge feeding mechanism in rorqual whales that underlies their extraordinary foraging performance and gigantic body size.

feeding; kinematics; modeling; morphology; rorquals

Introduction

Baleen whales (Mysticeti) evolved from toothed whale ancestors 25–30 million years ago, ultimately giving rise to several extant families that are defined by extremely large body size and specialized filter feeding mechanisms (49). It is generally believed that the combination of these highly effective feeding strategies and rising ocean productivity over the past 3 million years led to the extraordinary gigantic body sizes that are observed among extant mysticetes (58). Rorqual whales (Balaenopteridae), which include the largest species on earth, blue whales (*Balaenoptera musculus*) and fin whales (*Balaenoptera physalus*), employ a filter feeding mode called lunge feeding in which small-bodied, aggregated prey are first engulfed along with the water they are dispersed in, followed by the expulsion of the latter out of the buccal cavity via through-baleen filtration. Most interestingly, this two-step feeding mode is unique to rorquals and within the wider group of vertebrate filter feeders that feed by continuous and simultaneous engulfment and filtration.

Lunge feeding is facilitated by many anatomical specializations that have made it a highly dynamic feeding process. It consists of *1*) a rapid forward acceleratory lunge, *2*) lowering the mandibles to a gape of up to 80°, exposing the floor of the mouth to oncoming flow, *3*) engulfment of an enormous quantity of water along with small prey into the highly expansible ventral oropharyngeal cavity, *4*) mouth closing and filtration through the baleen plates, *5*) swallowing the retained prey; all of this in ~20–90 s (20, 28). Until the late 1980s, this spectacular behavior remained unexplored in any quantitative manner. Our current understanding of the physiology and biomechanics of rorqual lunge feeding is built on a foundation of anatomy and tissue biomechanics merged with kinematics data from whale-borne recording devices and mathematical modeling. Here, we present an integrative view of our current understanding of lunge filter feeding and pose key questions for future exploration.

Beginning in the 18th century (3, 7, 30, 33, 39, 40, 52, 59), morphologists have described and remarked on the high extensibility and elasticity of the pleated ventral groove blubber layer (VGB), which is the ventral wall of the engulfment cavity, and speculated on its role in lunge feeding mechanics. Orton and Brodie (38) tested postmortem tissue samples from fin whales and showed that the VGB was highly elastic and could be stretched by >1.5 times in the longitudinal axis, parallel to the grooves, and by >4 times transversely. They demonstrated that this elasticity was based on the presence of a high volume-fraction of thick elastin fibers embedded in the collagen and lipid matrix, in contrast to blubber on the rest of the body, which has high collagen content and virtually no elastin. Orton and Brodie (38) predicted that dynamic pressure from forward swimming would be needed to drive the engulfment process by inflating the ventral cavity with water, thus transforming the whale shape from highly streamlined to one resembling a "bloated tadpole." Subsequent field observations by Croll et al. (12) using barbed depth recorders shot into the blubber of whales with a crossbow revealed that dive times during lunge feeding for blue and fin whales averaged 5–7 min, that is, well below their theoretical aerobic dive limit of ~30 min (1, 11, 12) This led to a hypothesis that lunge feeding behavior is energetically expensive, particularly due to the rapid acceleration and high drag associated with the open mouth. But this also presents the paradoxical conclusion that the highly specialized feeding behavior that allows exploitation of pelagic prey aggregation so successfully also puts a severe limit on foraging times and

thus begs the question of feeding efficiency (energy gain ÷ energy expended) that will be addressed below.

Lunge Feeding Kinematics

The development of high-resolution digital multi-instrument tags, attached to the back of a whale by suction cups (6, 31), made it possible to record long-duration bouts of dive and lunge feeding behavior using sensors for depth, orientation, and audio. In the first such study on fin whales, Goldbogen and colleagues (17, 21) documented a rapid descent (gliding up to 6 m/s) at steep angles (>50°), initially powered by strong tail fluke strokes to overcome their positive buoyancy in the upper 50 m, then gliding to the depth of the prey patch (~250 m) in under 2 min. Typically, after a brief deceleration and re-orientation upward, lunges occurred along 5- to 20-m trajectories into the prey (from below the patch) with a fluke-powered acceleration to ~3 m/s, followed by mouth opening and rapid deceleration to near zero velocity as the water was engulfed and the mouth closed. After an average of 4.5 lunges, spaced ~45 s apart, the whales returned to the surface with powered swimming at steep angles (>60°) for a series of recovery breaths (see FIGURE 1). Subsequent studies on humpback (*Megaptera novaeangliae*) and blue whales revealed similar kinematic patterns with some differences related to body size (FIGURE 1) (19, 22, 23). Humpbacks, at a mean length of ~14 m, compared with 20 m for fins, had shallower feeding dives (140–160 m) with similar durations (7–8 min), but more lunges per dive (6–8 lunges). Blues, at an average of 25 m, dove to >200 m for ~10 min, but with fewer lunges per dive (2–5 lunges). These results suggest that body size is important and that the scale dependence of the lunge feeding mechanism has important consequences for rorqual physiology and ecology.

Lunge feeding is a dynamic and unsteady process involving fairly rapid changes in speed and heading for such large body masses (up to 200,000 kg), and performance is expected to decrease at larger geometrically similar body size due to the mismatched scaling of fluke and flipper area over body mass (66). However, the engulfment apparatus and capacity in rorquals does not scale with geometric similarity, as may be expected, but exhibits positive allometry, especially with respect to the skull and ventral oropharyngeal cavity (FIGURE 2A) (21, 23). The latter is crucial since it implies that lunging energy expenditures increase with body size when feeding on a common prey type (i.e., krill). But this feeding mode "works" despite incurring greater energy costs and necessitating greater power input for engulfing larger gulps (see *Modeling of Hydrodynamics and Energetics* below, and Refs. 23, 44). If true, the hyperallometry of lunge feeding costs may explain the short dive durations of the largest rorquals and the observation that the maximum number of lunges per dive decreases with body size (16, 23). In terms of lunge feeding performance, there appears to be a scale-dependent trade-off between engulfment capacity and diving capacity. Although the ability to dive longer and deeper should increase with body size because larger breath-holding animals can store more oxygen and also use oxygen at a lower mass-specific rate over time (29), the disproportionate energy invested in relatively larger gulps appears to progressively limit dive time in rorquals with increasing body size (23).

Engulfment capacities are extraordinary. Early estimates used a geometric model based on the allometry of the engulfment apparatus (21), and Kahane-Rapport and Goldbogen (32) estimated engulfment capacity to range from 500 liters in 5-m-long minke whales (*Balaenoptera acutorostrata*) to over 150,000 liters in 28-m-long blue whales. To take these larger gulps, the maximum lunge speeds appear to range from 2 to 4 m/s in adult humpback whales and from 3 to 4.7 m/s in adult blue whales (8, 19, 22, 23). Typical speed profiles during lunges consist of an acceleration to maximum speed followed by a much more rapid deceleration (FIGURE 2B). Tags equipped with cameras and inertial sensors demonstrate that whales generally open their mouths at maximum speed, whereas mouth closure occurs several seconds later after the body has lost much of its speed (8). The decrease in speed during engulfment is attributed to the increase in drag associated with flow around an open mouth at high speed (bluff body drag) as well as the additional drag generated as the engulfed water is accelerated forward from rest (engulfment drag) (41). After mouth closure, whales maintain very slow speeds of 1 m/s or lower as the engulfed water is purged from the oropharyngeal cavity and filtered by the baleen that hangs vertically from each side of the rostrum (28, 70). After the engulfed water is completely filtered and the retained prey swallowed, whales may perform additional lunges while at depth (28).

Although tag data show that maximum lunge speeds generally increase with body size, more detailed models of engulfment (see below) suggest that much lower speeds should be sufficient to create the dynamic pressure needed to inflate the ventral cavity, so it is not clear why such high speeds are used. One explanation could be related to the minimum speed necessary to overcome the escape speeds of targeted prey (42). Another explanation is that rorquals may engulf on momentum, i.e., with some assist from fluking (57), or coasting

for the most part (46), to minimize the mechanical cost of lunge feeding. As a result, faster speeds may be needed to prevent the larger whales from coming to a complete stop part way during engulfment. Fluking dynamics and associated speed profiles do not unambiguously support this hypothesis (17, 19, 22, 57), although higher-resolution tag technology may be able to test this question more rigorously in future work (8, 9).

The interplay between whale size and prey type likely has an important role in shaping the energetics of foraging in rorquals. As whale size increases, maneuvering performance predictably decreases due to the scaling of control surfaces relative to body volume. Surprisingly, tag data have revealed a wide range of maneuvers during lunge feeding. These include 180° rolls coupled with 90° pitching maneuvers to attack krill patches from below (28, 54), as well as complete 360° barrel rolls (24). Interestingly, mouth opening occurs at the apex of these rolling moments (28, 54). The anteriorly placed control surfaces (i.e., the wing-like flippers) can generate asymmetrical lift forces not only can rotate the body (53, 54) but also can be synchronized and canted upward to balance the downward (ventral) torque that occurs during mouth opening (10, 28). Whales appear to maneuver more when prey is less dense and more dispersed in smaller patches, which contrasts from relatively less maneuvering when foraging on deep and dense patches, so it is hypothesized that these acrobatic maneuvers are required to increase the proportion of patch that is engulfed (23, 25, 27).

Modeling of Hydrodynamics and Energetics

The intractability of performing laboratory-based investigations on living rorquals led to the formulation of hydrodynamic models of engulfment that, by incorporating field kinematics data and mor-

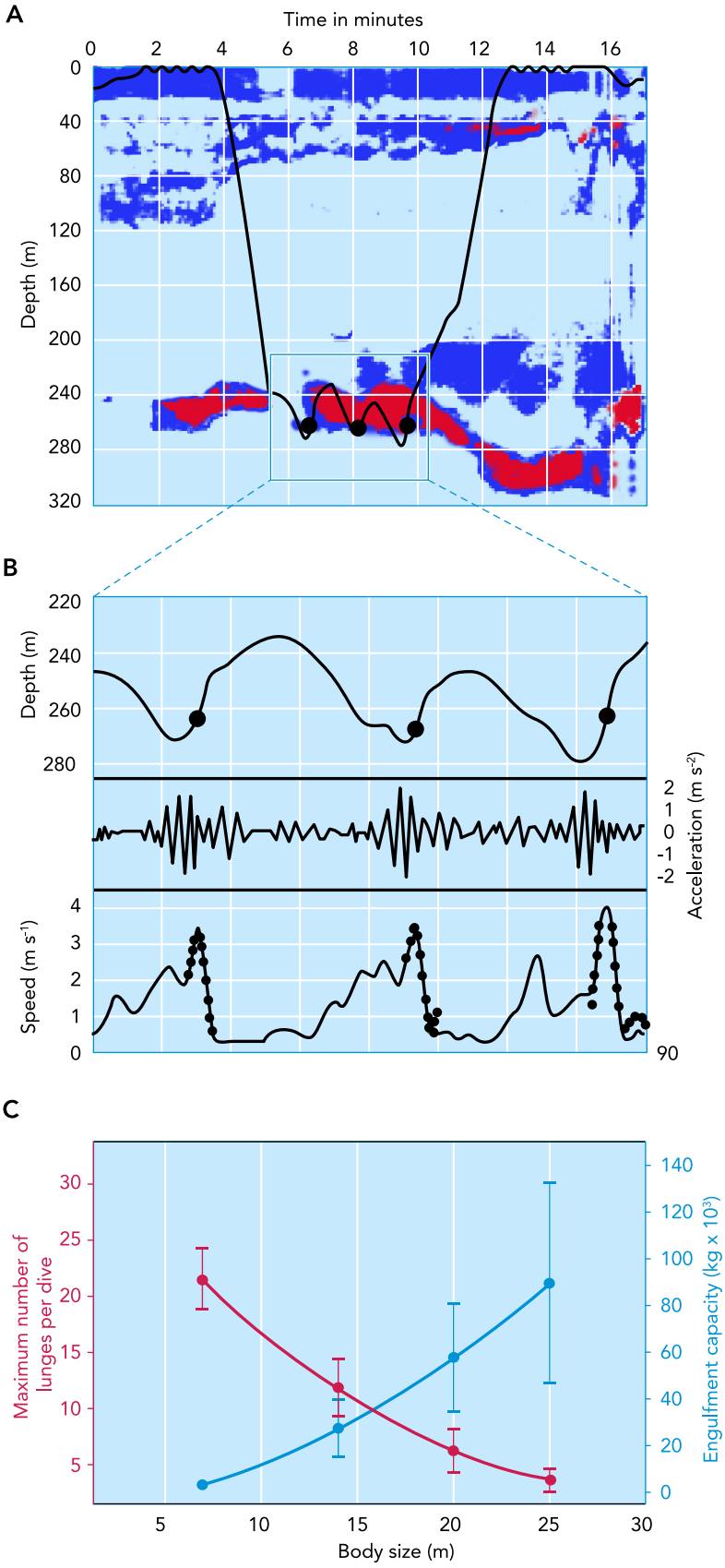

FIGURE 1. **Representative kinematics of lunge feeding**
A: dive profile (black line), with three lunges highlighted (black circles), superimposed on a prey field map that shows qualitative changes in krill density (light blue = low; blue = medium; red = high). *B*: detailed kinematics of the three lunges shown in *A*. Acceleration and fluking strokes are derived from accelerometer data. The speed trace is estimated from flow noise and confirmed by the superimposed black circles that show speed calculated from the vertical velocity of the body divided by the sine of the body pitch angle, also derived from accelerometers. Contents of *A* and *B* are from Ref. 22, with permission from the *Journal of Experimental Biology*. *C*: maximum number of lunges per dive and engulfment capacity plotted relative to average body length for four rorqual species (from smallest to largest: minke, humpback, fin and blue). Content from Ref. 16, with permission from the *Journal of Experimental Biology*.

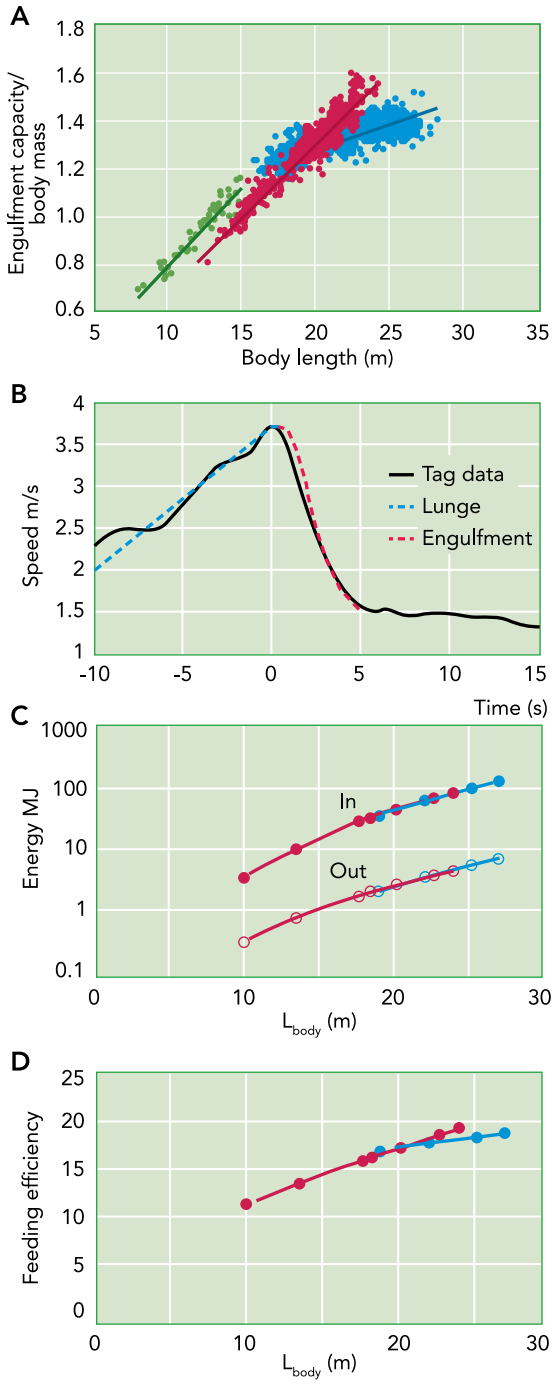

FIGURE 2. Modeling engulfment capacity and lunge energetics

A: engulfment capacity per kilogram of estimated body mass, plotted as a function of body length, for humpback (green symbols), fin (red symbols), and blue (blue symbols) whales (from Ref. 23). *B*: speed data from a digital tag on a 22.1-m fin whale (black line; Ref. 8), showing the acceleration into a lunge and the deceleration during engulfment, starting with mouth opening initiated at reference time = 0. Simulated speed profile for this lunge (broken lines) shows good agreement with the tag data (calculated using the model in Ref. 44). This model allows calculation of drag forces, work done, and energy expended. *C*: comparison of energy obtained from captured prey (In) and energy expended for engulfment (Out), for blue (blue dots) and fin (red dots) whales, with typical approach speed of 3 m/s and krill density of 0.2 kg/m^3. *D*: feeding efficiency calculated as the ratio of energy gain to energy expended from *C*.

phological measurements in fin, humpback, and blue whales, have produced quantitative estimates—and even predictions—of the drag forces at play and the ensuing metabolic expenditures (FIGURE 2B) (18, 21, 42, 44). In particular, this modeling suggests a tight relationship between the initial speed and the rate of mouth opening and deceleration, predicting that inflation of the ventral cavity inflation is actively controlled by the musculature underlying the VGB layer (41, 55) rather than passively by dynamic pressure and VGB elasticity alone, as previously thought (33, 38). The active role for muscle in the ventral cavity wall (i.e., "active engulfment") was postulated as a mechanism to accelerate water forward early during engulfment, resulting in significant reductions in structural loads sustained by the body. In a "passive engulfment" scenario, where elastic stresses are weak and the VGB is "compliant" and where VGB muscle is activated only to prevent being overstretched (55), such loads would occur at the very end and with greater force, similar to inflating plastic bags swiftly flung around through the air (or water). How much muscle force is generated, and during which part of the engulfment process (i.e., early, throughout, or only at the very end) still requires further study (55).

Linking the mechanics of engulfment and filtration to metabolic expenditures is done by considering the energy expended by the tail and VGB musculature during *1*) the fluking-propelled accelerative approach to the prey aggregation; *2*) engulfment itself, which translates into a loss of speed by the rorqual due to cessation of fluking, along with a gain of speed by the engulfed mass as momentum is robbed from the whale; and *3*) the expulsion of the engulfed water out of the cavity via through-baleen filtration. Although still lacking many details (70), purging/filtration is the longest of the three stages and is suspected to incur the smallest power expenditures. On the other hand, the first (accelerative) stage is likely the most expensive, metabolically incurring between 10 and 60 J/kg of body mass (assuming minimal drag losses by a highly streamlined body), or up to 6,000 kJ for a 100,000-kg, 26-m blue whale, and at a power output of ~0.6 MW when accelerating over time scales of ~10 s.

Energetic expenditures during engulfment are reasonably well understood, at least for the medium to very large species (humpback to blues), as generated by the VGB musculature pushing the engulfed mass forward to compensate for the low tissue elastic potential energy accumulated during its stretching, i.e., over strain values (55) that correspond to very low elastic stresses (38). Assuming exclusive VGB muscle use (rather than passive elasticity), and noting the speed decrement during

engulfment matching approximately the speed increment of the accelerative approach toward the prey (and corresponding changes in kinetic energy), yields expenditures that are quantitatively similar to those of the prey approach stage. Finally, and assuming purging/filtration to run at near resting metabolic rates, one arrives at metabolic expenditures of 5–8 MJ during single lunges performed by blue whales in the 25- to 27-m upper body size range (22). Calculating energy expenditures by the smaller rorquals such as the minke whale are uncertain at this point since the low VGB elastic stresses generated during engulfment may be enough to set the engulfed mass into motion and at the speeds observed in the field compiled in tag studies (Cade et al., 57).

The seemingly high energetic cost of lunge feeding turns out to be favorable to large body size because of the scaling in morphological adaptations that has increased the overall feeding efficiency at such sizes. This is seen with the scaling of engulfment capacity, which exhibits positive allometry with respect to body mass, i.e., increasing disproportionately in larger animals due to relatively greater head size but only partly offsetting the adverse energetic effects of getting larger (21). Head width, jaw length, and VGB length in fin whales, derived from morphometrics, all increase relative to body length with exponents of 1.15, 1.24, 1.14, respectively [although geometric similarity, i.e., isometry, predicts length exponents of 1.0 (or "iso" = 1)]. Projected mouth area scales as the product of head width and jaw length, with an exponent of 2.39 (iso = 2) (21). Modeling predicted engulfment capacities in humpback, fin, and blue whales to increase with respective length exponents of 3.21, 3.51, and 3.65 (iso = 3), and mass-specific engulfment capacities had length exponents of 0.86, 0.94, and 0.37 (iso = 0) (FIGURE 2A) (23). The posterior portion of the body involved in propulsion grows with negative allometry (i.e., with body length exponents < isometry), whereas the propulsive surfaces scale isometrically. Consequently, larger whales can engulf relatively greater volumes of water, but at increasing drag energy costs (FIGURE 2C). Interestingly, field studies suggest a rather weak relationship between the speed at mouth opening before engulfment and body size (8, 46). Metabolic and propulsive energetic expenditures follow the increase in kinetic energy during prey approach and scale primarily with body mass. Energy gain from prey engulfment increases faster than energy expended with increasing body size (FIGURE 2C); thus feeding efficiencies for a given prey density are predicted to increase in larger whales (FIGURE 2D). Because lunge feeding energy expenditure allometry is positive whereas lunge feeding duration allometry is negative, overall required power output is expected to quickly increase with body size, suggesting that physics ultimately limits the maximum body size for successful lunge feeding (44). Although the extreme hydrodynamic drag associated with engulfment sets a high energetic cost, the very high feeding efficiency actually makes this behavior feasible and likely the only method that could sustain such large body size. With engulfment involving short bouts of high-intensity muscle activity, the metabolic model also shows a size limit such that, above 30 m (the maximum for extant blue whales), the mass-specific instantaneous power for required lunge speed is not available. More importantly, reduced mass-specific lunge power at small sizes may allow weaned juveniles to begin lunge feeding at low metabolic cost and to achieve rapid growth. Lower power for engulfment at smaller body sizes may also have implications for how lunge feeding evolved in smaller ancestral baleen whales.

Anatomical Specializations That Support Lunge Feeding

Despite decades of sustained hunting that provided countless opportunities for scientific discovery, details of the anatomy and physiology of baleen whales have largely remained obscure. Arguably the most prominent and significant features related to lunge feeding are the large mandibles and highly distensible and elastic ventral cavity and its constituent components (FIGURES 3 AND 4). Recent studies on anatomy and mechanics of these structures from postmortem specimens of rorquals have yielded insight and inference about the biomechanical aspects of lunge feeding (26). Rorqual mandibles are large, making up 20–25% of total body length (47), and are reinforced with dense compact bone to support bending loads associated with lunging (FIGURE 3, A AND B) (14, 56). They are curved and rotate outward (laterally) to increase the projected mouth width during engulfment (4, 5). This mobility is possible due to specialized fibrous elastic ligaments at the temporomandibular joints (i.e., the jaw hinge) (2, 30, 34, 39, 52) and an unfused mandibular symphysis (the chin) (FIGURE 3, A AND C) (34, 48).

An additional and unusual feature that may help control jaw opening is referred to as the frontomandibular stay (34), likened to the check ligaments in the lower limbs of horses. It is an elastic fibrous linkage (primarily composed of elastin and collagen) between the frontal bone of the skull and the coronoid process of the mandible. It is hypothesized to act in parallel with the temporalis muscle, being stretched and storing elastic energy from jaw opening, and recoiling to help power closing while also protecting the temporalis from over-extension (34). Water forced into the mouth during a lunge moves back into the expanding ventral cavity that

opens between the VGB layer and the underlying body wall. The floor of the mouth and tongue stretch and slide along a fascial layer to become the lining of the enormous cavity (21, 33, 39, 67, 70), which extends caudally by 50–60% of the body length.

The VGB wall comprises a dermal furrowed blubber layer and underlying longitudinal and oblique skeletal muscle strata, all of which are heavily invested with robust collagen and elastin fibers (FIGURE 4, F AND G) (38, 55, 59), in contrast to other skeletal muscles. The extreme distension of the VGB during engulfment suggests strains that are implausible for the physiological limits of vertebrate skeletal muscle. The solution is that the VGB muscles, which run either along or at 45° to the longitudinal body axis, have a folded configuration in the relaxed state that accommodates expansion to the predicted full engulfment with muscle strains of ~20–50%, whereas parallel elastin fibers help in recovery to the relaxed length (55) when the water is purged. Interestingly, nerves within the tongue and VGB appear exceptionally stretchy and elastic (FIGURE 4A); some reversibly extensible to >100% (FIGURE 4, B AND C) (64). Micro-CT and microscopy show a highly folded core of parallel nerve fascicles inside a thick sheath, again containing elastin and wavy collagen fibers (36, 64). (FIGURE 4, D AND E). In this arrangement, the core and fascicles unfold when the sheath is stretched to a limit set by the stiff collagen, protecting the nerve from stretch damage. Recoil of the sheath restores fascicle folding in a manner that minimizes bending strain on fascicle elements. Constituent blood vessels are also highly elastic and accommodate VGB expansion, not surprisingly, by reliance on a high content of elastin fibers (Lillie MA, unpublished observations).

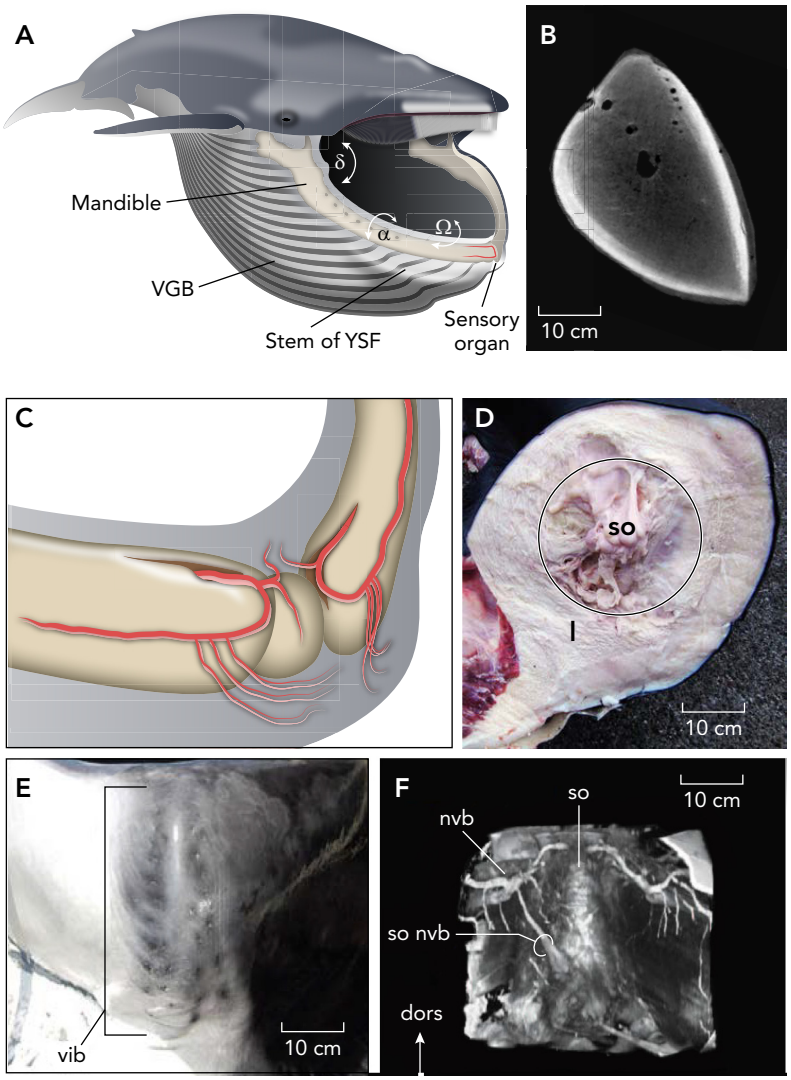

FIGURE 3. **Anatomy of the mandible and sensory organ**
A: rorquals have large mandibles that rotate in three axes when lunge feeding to increase mouth opening area. Lowering the mandible increases angle δ at the temporomandibular joint, widening of the mouth by lateral rotation of the mandible increases α, and lateral separation at the temporomandibular joint causes rotation Ω at the mandibular symphysis. *B*: CT scan of a fin whale mandible at about mid-shaft, showing high-density cortical bone (bright) in a thin peripheral layer and low-density trabecular bone (dark) throughout the remainder. *C*: location of the sensory organ in the mandibular symphysis of a fin whale with neurovascular supply arising from the mandibular canals. *D*: midline sagittal section through the sensory organ (*so*, black outline), also showing the ligamentous tissue (l). *E*: chin of a fin whale showing the sensory bristles (dark pits) external to the sensory organ. MRI of the chin revealing the neurovascular bundles (nvb) supplying the sensory organ (so). *A*, *C*—*F* are based on Ref. 48, with permission from *Nature*. B is from Ref. 56, with permission from *Anatomical Record*.

Outward rotation of the mandibles is also facilitated by the flexible ligament that connects the unfused mandible tips. Within this ligament, Pyenson et al. (48) found a putative sensory organ that may help control jaw motion (FIGURE 3). This organ is a collection of small papillae suspended in a gel-like matrix, with blood vessels and encapsulated nerve endings derived from branches of the mandibular branch of the trigeminal nerve (cranial V) (65). Interestingly, these neurovascular bundles emerge from vestigial foramina of the jaws, a structure that is homologous with the anterior-most tooth socket in ancestral "toothed" mysticetes, suggesting its evolutionary origin may be related to loss of teeth and emergence of baleen. It seems likely that this mechano-sensor is stimulated by changes in jaw configuration during engulfment, when rotation of the jaws will deform the symphysis and the sensory organ, which communicates with the brain (48). It may also be sensitive to expansion of the VGB by connection to the Y-shaped fibrocartilage embedded in the VGB at the anterior end of the engulfment cavity (YSF; see FIGURE 3A) (39). This discovery of the "chin" organ provides the anatomical basis for sensory control over the rate of jaw opening and water engulfment during lunge-feeding, as predicted by dynamic models (see above), and it sheds light on the possible evolutionary sequence of key traits that allowed rorqual whales to become lunge feeders and ultimately the largest vertebrates on earth.

Future Perspectives

Filtration Styles

Although a detailed understanding of lunge-feeding biomechanics and physiology is emerging, driven by advances in animal-borne sensors, video technology, and anatomical discoveries, many fundamental questions remain, some more intractable than others. One of the most intriguing and critical aspects of lunge feeding that is still a mystery is the process of filtration and swallowing of prey. With the baleen plates arranged in long parallel racks on each side of the mouth, one might imagine that water is simply forced laterally through the gaps as the VGB contracts, leaving the prey inside the mouth. However, filtration is rapid and flow rates are high. For example, a 20-m fin whale may filter ~2.5 m^3 of water per second, flowing at a velocity of 0.8 m/s through the baleen plates (18). A "sieve" type of filtration is improbable since it would undoubtedly cause prey to be lodged into the layer of fine fringes on the inner surface of the plates with no obvious way to recover it.

How the baleen plates and the mouth cavity create a mechanism to expel water, retain their prey without clogging the filter, and then collect it into a bolus that is forced past the oral plug and into the oropharynx is an open question. Cross-flow filtration has been proposed for balaenids (e.g., right and bowhead whales) (45, 68) that feed on small copepods by using a continuous flow of water along the inside of the baleen from anterior to posterior such that prey is diverted as the water leaks out through the baleen. But the rorqual anatomy and larger prey size do not seem suited to this mechanism. Werth and Ito (69) hypothesized that three anatomical components of the mouth act together to manipulate the prey and guide it to the back of the oral cavity after the water has been expelled. In their model, accumulated prey would be pushed up and back by elevated lingual muscles and funneled medially as it passed between the narrowing posterior ends of the baleen racks. In addition, the residual water in the bolus could escape through a channel formed at the posterior margin of the lip (69). This is an intriguing hypothesis that may be testable if animal-borne cameras can be deployed in positions to record flow events during filtration.

Detection of the Prey

Another important aspect of rorqual feeding that needs to be investigated is how prey patches are detected. There are multiple temporal and spatial scales to this problem. The most basic question relates to how whales find food at the ocean basin scale in a generally featureless ocean offshore. Long-term tag data demonstrate that blue whales track a 10-yr average of oceanic productivity better than contemporaneous conditions, suggesting that memory helps drive migrations to foraging grounds in the summer months. However, once whales arrive at known feeding areas, how do they find food that is frequently deep in the water column? Chemoattraction to algal-derived dimethyl sulfide, as observed in other marine vertebrates, may enable rorquals to find food (see Ref. 51). Some whales may perform what is interpreted as

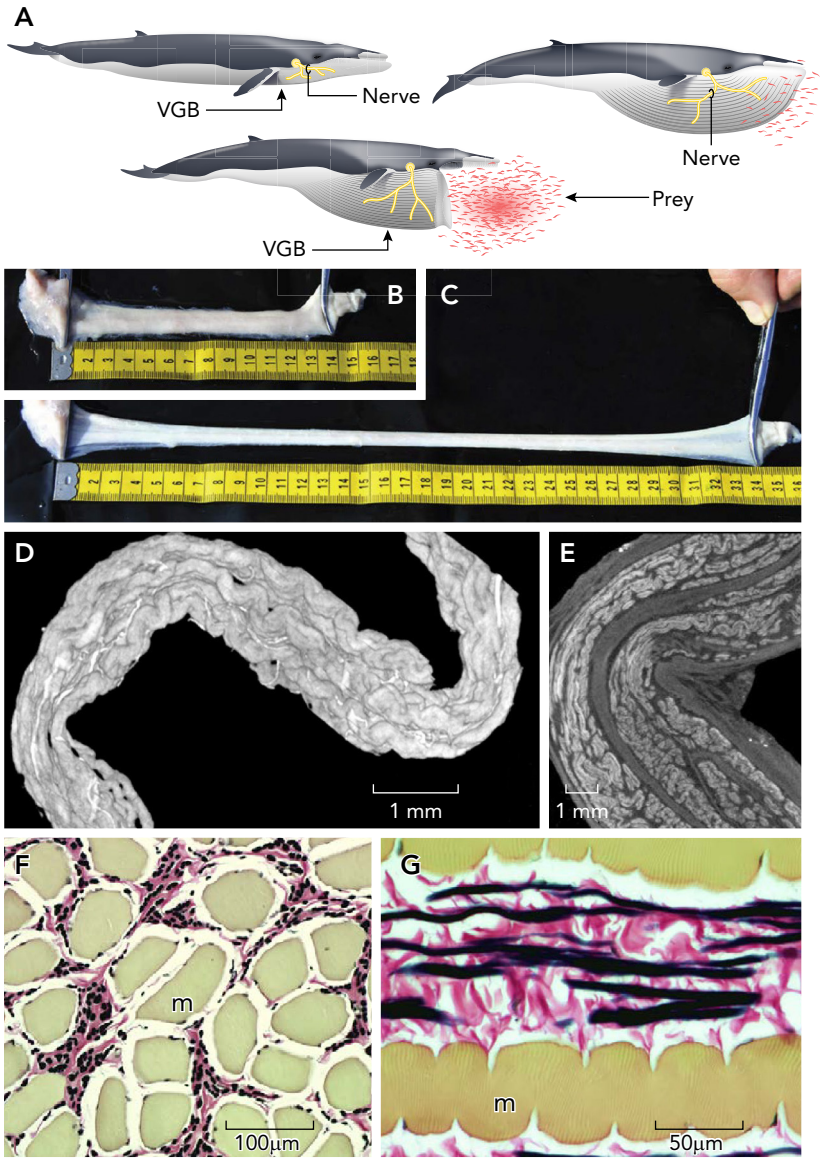

FIGURE 4. **Anatomy of stretchy nerves and muscle in the ventral groove blubber**
A: the nerves (yellow) in the VGB stretch as the ventral cavity expands during a lunge. Segment of a nerve before (*B*) and after extending by >100% (*C*). *D*: 3D reconstruction from micro-CT scans of a VGB nerve showing two levels of folding. *E*: nerve fascicles are relatively straight at outer curvature of core bend and very wavy at inner curvature. *F*: cross section of muscle cells (m) of the VGB, showing dense array of elastin fibers (black) among the collagenous connective tissue (pink). *G*: longitudinal section of VGB muscle showing high degree of folding with straight elastin fibers. *A*—*C* are from Ref. 64, with permission from *Current Biology*. *D* and *E* are from Ref. 36, with permission from *Current Biology*. *F* and *G* are from Ref. 55, with permission from the *Journal of Experimental Biology*.

test dives or search dives, V-shaped dives at the initiation of a feeding bouts (15). Such a behavior may indicate that rorquals dive deep until they can visually detect prey patches. Interestingly, searching dives in humpback whales located in the western Antarctic Peninsula occur before dusk, and feeding continues through the night. Nighttime feeding has also been observed in other species, such as blue whales in St. Lawrence (13), and may suggest that other sensory modalities are used to find prey. Rorquals exhibit two rows of sensory hairs or vibrissae on the anterior aspect of the chin that connect to a unique sensory organ (FIGURE 3, E AND F) (48). Such a system may be used in a tactile sense to register contact with a prey field and provide sensory information for rorquals to open their mouths at the greatest prey density in low-light conditions. Lastly, echo-ranging acoustic behavior (as opposed to echolocation at higher frequencies) has been recorded by tags deployed on humpback whales foraging at night (60) but has not been recorded subsequently despite the large number of tagging studies on this species.

Bio-hydrodynamic Questions

Continued development of hydrodynamics models should be the best approach to improve our understanding of engulfment dynamics. The active engulfment hypothesis should be tested more thoroughly to determine whether engulfment always involves activated VGB muscle or whether it may be entirely passive (i.e., with no muscular control of VGB expansion), and whether species with different body sizes or with different prey targets (krill versus fish) influence this. Clearly, gape-angle changes are actively controlled, so one can wonder whether gape alone sets the engulfment volume or whether other factors are at play. Other outstanding questions revolve around the timing of mouth opening to maximize prey capture, and in conjunction with varying light conditions and prey types. The morphology of the VGB and its muscle layers deserve further study in relation to scaling with body size among species and to determine whether differences in VGB composition influence engulfment dynamics. A related issue is the strain rate of the VGB inflation and the corresponding changes in speed during engulfment. Data on these aspects will be important for assessing how much elastic energy is provided by elastin fibers in the VGB and muscle to help expel water. An interesting case could be that of bubble-net feeding by adult humpback whales in which engulfment done on a vertical trajectory at the sea surface appears to be unassisted by active VGB muscle pushing the engulfed water. (This inference is based on observations that, as the mandibles break the surface, the water contained does not noticeably move above the sea surface.) Further research into whale metabolism is urgently needed to inform energetics models and soon may be supported with the development of new digital tags that can measure physiological indicators, such as heart rate and, hopefully one day, blood pressure.

Modeling simulations that make use of computational fluid dynamics (CFD) techniques will be an important next step in understanding the fluid forces acting on rorquals when swimming and lunging, which can then inform and refine energetics models. So far, initial studies have focused on pectoral fins and effects of the ventral grooves on drag reduction (37, 61, 62). But complete—and time-dependent—CFD simulations should be expected only in the long term. Lunge feeding is an unsteady process in which the whales and co-moving fluids accelerate and decelerate sequentially. Moreover, the hydrodynamic problem becomes difficult to solve because the fluid interacts with a structure that is changing in shape and volume over time (requiring mesh body-fluid boundaries that are updated at each iterative step). Finally, further and complex fluid-structure interactions are expected along with large-scale turbulence during the deceleration portion of a lunge when a whale's wake catches up and collides with the body. Very much like parachute inflation (43), modeling the fluid flows of a lunge will require significant computer power and expertise. Finally, and to further exacerbate the difficulty of this endeavor, characterizing the details of body shape of a 20-m-long animal, along with the elastic properties of several relevant body parts (such as the VGB and flukes) cannot be accomplished in a laboratory setting as routinely done with fish (e.g., Refs. 35, 63). Similar to the aircraft aerodynamics and performance analysis tools of the past, the use of simpler methods that capture enough features to be relevant and predictive will remain the main analysis tool for the foreseeable future.

Potential Impact of Climate Change

With the ever-increasing concern about global climate change, it may be of interest to consider the impact of these changes on populations of rorqual whales from the perspective of lunge-feeding energetics. These are large organisms with high mobility in the ocean that routinely travel great distances between summer feeding grounds at high latitudes and winter ranges at lower latitudes. Reduction of krill density or aggregations is a key factor that could negatively impact growth and survival of rorquals. In particular, blue whales are obligate krill specialists that rely on dense patches to obtain sufficient energy intake. Some climate change scenarios suggest average sea surface temperature increases of up to 6°C this century (50)

and a model study of changes in top predator species distribution based on climate models predicted that blue whale habitat in the eastern North Pacific could decease by 15% or more (29a). Although it is not clear how these changes might affect krill availability, we can predict a linear inverse relationship between krill density and feeding efficiency. For example, at a krill density of 0.2 kg/m^3, a 25-m blue whale could achieve a feeding efficiency of ~18 (FIGURE 2D), but this would drop to 6 if krill density fell by a factor of 3, and to only 2 at a density reduction of 9. Thus, if climate change decreases the density and or summer persistence of critical krill patches and blue whales are unable to make up the deficit with longer feeding efforts, then their populations may suffer declines. ■

R.E.S. thanks the Natural Sciences and Engineering Research council of Canada for ongoing grant support; J.P. is supported by a grant from the National Science Foundation (NSF) (IOS-1656656); J.A.G. is supported in part by grants from the NSF (IOS-1656676), the Office of Naval Research (N000141612477), and a Terman Fellowship from Stanford University.

No conflicts of interest, financial or otherwise, are declared by the author(s).

R.E.S., J.P., and J.A.G. interpreted results of experiments; R.E.S. prepared figures; R.E.S., J.P., and J.A.G. drafted manuscript; R.E.S., J.P., and J.A.G. edited and revised manuscript; R.E.S., J.P., and J.A.G. approved final version of manuscript; J.A.G. analyzed data.

References

1. Acevedo-Gutiérrez A, Croll DA, Tershy BR. High feeding costs limit dive time in the largest whales. *J Exp Biol* 205: 1747–1753, 2002.
2. Arnold PW, Birtles RA, Sobtzick S, Matthews M, Dunstan A. Gulping behaviour in rorqual whales: underwater observations and functional interpretation. *Mem Queensl Mus* 51: 309–332, 2005.
3. Brodie PF. Form, function and energetics of cetacea: a discussion. In: *Functional Anatomy of Marine Mammals*, edited by Harrison RJ. New York: Academic Press, 1977, p. 45–56.
4. Brodie PF. Noise generated by the jaw actions of feeding fin whales. *Can J Zool* 71: 2546–2550, 1993. doi:10.1139/z93-348.
5. Brodie PF. Feeding mechanics of rorquals *Balaenoptera* sp. In: *Secondary Adaptations of Tetrapods to Life in Water*, edited by Mazin JM, de Buffrenil V. Munchen, Germany: Verlag Dr. Freidrich Pfeil, 2001, p. 345–352.
6. Burgess WC, Tyack PL, Le Boeuf BJ, Costa DP. A programmable acoustic recording tag and first results from free-ranging northern elephant seals. *Deep Sea Res Part II Top Stud Oceanogr* 45: 1327–1351, 1998. doi:10.1016/S0967-0645(98)00032-0.
7. Carte A, Macalister A. On the anatomy of *Balaenoptera rostrata*. *Philos Trans R Soc Lond, B* 158: 201–261, 1868. doi:10.1098/rstl.1868.0009.
8. Cade DE, Friedlaender AS, Calambokidis J, Goldbogen JA. Kinematic diversity in rorqual whale feeding mechanisms. *Curr Biol* 26: 2617–2624, 2016. doi:10.1016/j.cub.2016.07.037.
9. Cade DE, Barr KR, Calambokidis J, Friedlaender AS, Goldbogen JA. Determining forward speed from accelerometer jiggle in aquatic environments. *J Exp Biol* 221: jeb170449, 2018. doi:10.1242/jeb.170449.
10. Cooper LN, Sedano N, Johansson S, May B, Brown JD, Holliday CM, Kot BW, Fish FE. Hydrodynamic performance of the minke whale (*Balaenoptera acutorostrata*) flipper. *J Exp Biol* 211: 1859–1867, 2008. doi:10.1242/jeb.014134.
11. Croll DA, Tershy BR, Hewitt RP, Demer DA, Fiedler PC, Smith SE, Armstrong W, Popp JM, Kiekhefer T, Lopez VR, Urbán J, Gendron D. An integrated approach to the foraging ecology of marine birds and mammals. *Deep Sea Res Part II Top Stud Oceanogr* 45: 1353–1371, 1998. doi:10.1016/S0967-0645(98)00031-9.
12. Croll DA, Acevedo-Gutiérrez A, Tershy BR, Urbán-Ramírez J. The diving behavior of blue and fin whales: is dive duration shorter than expected based on oxygen stores? *Comp Biochem Physiol A Mol Integr Physiol* 129: 797–809, 2001. doi:10.1016/S1095-6433(01)00348-8.
13. Doniol-Valcroze T, Lesage V, Giard J, Michaud R. Optimal foraging theory predicts diving and feeding strategies of the largest marine predator. *Behav Ecol* 22: 880–888, 2011. doi:10.1093/beheco/arr038.
14. Field DJ, Campbell-Malone R, Goldbogen JA, Shadwick RE. Quantitative computed tomography of humpback whale (*Megaptera novaeangliae*) mandibles: mechanical implications for rorqual lunge-feeding. *Anat Rec (Hoboken)* 293: 1240–1247, 2010. doi:10.1002/ar.21165.
15. Friedlaender AS, Tyson RB, Stimpert AK, Read AJ, Nowacek DP. Extreme diel variation in the feeding behavior of humpback whales along the western Antarctic Peninsula during autumn. *Mar Ecol Prog Ser* 494: 281–289, 2013. doi:10.3354/meps10541.
16. Friedlaender AS, Goldbogen JA, Nowacek DP, Read AJ, Johnston D, Gales N. Feeding rates and under-ice foraging strategies of the smallest lunge filter feeder, the Antarctic minke whale (*Balaenoptera bonaerensis*). *J Exp Biol* 217: 2851–2854, 2014. doi:10.1242/jeb.106682.
17. Goldbogen JA, Calambokidis J, Shadwick RE, Oleson EM, McDonald MA, Hildebrand JA. Kinematics of foraging dives and lunge-feeding in fin whales. *J Exp Biol* 209: 1231–1244, 2006. doi:10.1242/jeb.02135.
18. Goldbogen JA, Pyenson ND, Shadwick RE. Big gulps require high drag for fin whale lunge feeding. *Mar Ecol Prog Ser* 349: 289–301, 2007. doi:10.3354/meps07066.
19. Goldbogen JA, Calambokidis J, Croll DA, Harvey JT, Newton KM, Oleson EM, Schorr G, Shadwick RE. Foraging behavior of humpback whales: kinematic and respiratory patterns suggest a high cost for a lunge. *J Exp Biol* 211: 3712–3719, 2008. doi:10.1242/jeb.023366.
20. Goldbogen JA. The ultimate mouthful: lunge feeding in rorqual whales. *Am Sci* 98: 124–131, 2010. doi:10.1511/2010.83.124.
21. Goldbogen JA, Potvin J, Shadwick RE. Skull and buccal cavity allometry increase mass-specific engulfment capacity in fin whales. *Proc Biol Sci* 277: 861–868, 2010. doi:10.1098/rspb.2009.1680.
22. Goldbogen JA, Calambokidis J, Oleson E, Potvin J, Pyenson ND, Schorr G, Shadwick RE. Mechanics, hydrodynamics and energetics of blue whale lunge feeding: efficiency dependence on krill density. *J Exp Biol* 214: 131–146, 2011. doi:10.1242/jeb.048157.
23. Goldbogen JA, Calambokidis J, Croll DA, McKenna MF, Potvin J, Pyenson ND, Schorr G, Shadwick RE, Tershy B. Scaling of lunge feeding performance in rorqual whales: mass-specific energy expenditure increases with body size and progressively limits diving capacity. *Funct Ecol* 26: 216–226, 2012. doi:10.1111/j.1365-2435.2011.01905.x.
24. Goldbogen JA, Calambokidis J, Friedlaender AS, Francis J, DeRuiter SL, Stimpert AK, Falcone E, Southall BL. Underwater acrobatics by the world's largest predator: 360° rolling manoeuvres by lunge-feeding blue whales. *Biol Lett* 9: 20120986, 2013. doi:10.1098/rsbl.2012.0986.
25. Goldbogen JA, Friedlaender AS, Calambokidis J, McKenna MF, Simon M, Nowacek DP. Integrative approaches to the study of baleen whale diving behavior, feeding performance, and foraging ecology. *Bioscience* 63: 90–100, 2013. doi:10.1525/bio.2013.63.2.5.
26. Goldbogen JA, Shadwick RE, Lillie MA, Piscitelli MA, Potvin J, Pyenson ND, Vogl AW. Using morphology to infer physiology: case studies on rorqual whales (Balaenopteridae). *Can J Zool* 93: 687–700, 2015. doi:10.1139/cjz-2014-0311.

27. Goldbogen JA, Hazen EL, Friedlaender AS, Calambokidis J, DeRuiter SD, Stimpert AK, Southall BL. Prey density and distribution drive the three-dimensional foraging strategies of the largest filter feeder. *Funct Ecol* 29: 951–961, 2015. doi:10.1111/1365-2435.12395.

28. Goldbogen JA, Cade DE, Calambokidis J, Friedlaender AS, Potvin J, Segre PS, Werth AJ. How baleen whales feed: the biomechanics of engulfment and filtration. *Annu Rev Mar Sci* 9: 367–386, 2017. doi:10.1146/annurev-marine-122414-033905.

29. Halsey LG, Butler PJ, Blackburn TM. A phylogenetic analysis of the allometry of diving. *Am Nat* 167: 276–287, 2006. doi:10.1086/499439.

29a. Hazen EL, Jorgensen S, Rykaczewski RR, Bograd SJ, Foley DG, Jonsen ID, Shaffer SA, Dunne JP, Costa DP, Crowder LB, Block BA. Predicted habitat shifts of Pacific top predators in a changing climate. *Nature Climate Change* 3: 234–238, 2013. doi:10.1038/nclimate1686.

30. Hunter J. Observations on the structure and oeconomy of whales. *Philos Trans R Soc Lond* 77: 371–450, 1787. doi:10.1098/rstl.1787.0038.

31. Johnson M, Tyack PL. A digital acoustic recording tag for measuring the response of wild marine mammals to sound. *IEEE J Oceanic Eng* 28: 3–12, 2003. doi:10.1109/JOE.2002.808212.

32. Kahane-Rapport SR, Goldbogen JA. Allometric scaling of morphology and engulfment capacity in rorqual whales. *J Morphol* 279: 1256–1268, 2018. doi:10.1002/jmor.20846.

33. Lambertsen RH. Internal mechanism of rorqual feeding. *J Mammalogy* 64: 76–88, 1983. doi:10.2307/1380752.

34. Lambertsen RH, Ulrich N, Straley J. Frontomandibular stay of Balaenopteridae: a mechanism for momentum recapture during feeding. *J Mammalogy* 76: 877–899, 1995. doi:10.2307/1382758.

35. Lauder GV, Lim J, Shelton R, Witt C, Anderson EJ, Tangorra J. Robotic models for studying undulatory locomotion in fishes. *Mar Technol Soc J* 45: 41–55, 2011. doi:10.4031/MTSJ.45.4.8.

36. Lillie MA, Vogl AW, Gil KN, Gosline JM, Shadwick RE. Two levels of waviness are necessary to package the highly extensible nerves in rorqual whales. *Curr Biol* 27: 673–679, 2017. doi:10.1016/j.cub.2017.01.007.

37. Miklosovic DS, Murray MM, Howle LE, Fish FE. Leading-edge tubercles delay stall on humpback whale (*Megaptera novaeangliae*) flippers. *Phys Fluids* 16: L39–L42, 2004. doi:10.1063/1.1688341.

38. Orton LS, Brodie PF. Engulfing mechanics of fin whales. *Can J Zool* 65: 2898–2907, 1987. doi:10.1139/z87-440.

39. Pivorunas A. The fibrocartilage skeleton and related structures of the ventral pouch of balaenopterid whales. *J Morphol* 151: 299–313, 1977. doi:10.1002/jmor.1051510207.

40. Pivorunas A. The feeding mechanisms of baleen whales. *Am Sci* 67: 432–440, 1979.

41. Potvin J, Goldbogen JA, Shadwick RE. Passive versus active engulfment: verdict from trajectory simulations of lunge-feeding fin whales *Balaenoptera physalus*. *J R Soc Interface* 6: 1005–1025, 2009. doi:10.1098/rsif.2008.0492.

42. Potvin J, Goldbogen JA, Shadwick RE. Scaling of lunge feeding in rorqual whales: an integrated model of engulfment duration. *J Theor Biol* 267: 437–453, 2010. doi:10.1016/j.jtbi.2010.08.026.

43. Potvin, J., Bergeron, K., Brown, G., Charles, R., Desabrais, K., Johari, H., Kumar, V., McQuilling, M., Morris, A., Noetscher, G. and Tutt, B. The Road Ahead: A White Paper on the Development, Testing and Use of Advanced Numerical Modeling for Aerodynamic Decelerator Systems Design and Analysis. In: 21st AIAA Aerodynamic Decelerator Systems Technology Conference and Seminar. 2011. doi:10.2514/6.2011-2501.

44. Potvin J, Goldbogen JA, Shadwick RE. Metabolic expenditures of lunge feeding rorquals across scale: implications for the evolution of filter feeding and the limits to maximum body size. *PLoS One* 7: e44854, 2012. doi:10.1371/journal.pone.0044854.

45. Potvin J, Werth AJ. Oral cavity hydrodynamics and drag production in Balaenid whale suspension feeding. *PLoS One* 12: e0175220, 2017. doi:10.1371/journal.pone.0175220.

46. Potvin J, Cade DE, Werth AJ, Shadwick RE, Goldbogen JA. Gigantism and the energetics of lunge-feeding baleen whales. *Am J Phys*. 2019.

47. Pyenson ND, Goldbogen JA, Shadwick RE. Mandible allometry in extant and fossil Balaenopteridae (Cetacea: Mammalia): the largest vertebrate skeletal element and its role in rorqual lunge feeding. *Biol J Linn Soc Lond* 108: 586–599, 2013. doi:10.1111/j.1095-8312.2012.02032.x.

48. Pyenson ND, Goldbogen JA, Vogl AW, Szathmary G, Drake RL, Shadwick RE. Discovery of a sensory organ that coordinates lunge feeding in rorqual whales. *Nature* 485: 498–501, 2012. doi:10.1038/nature11135.

49. Pyenson ND. The ecological rise of whales chronicled by the fossil record. *Curr Biol* 27: R558–R564, 2017. doi:10.1016/j.cub.2017.05.001.

50. Rosenzweig C, Karoly D, Vicarelli M, Neofotis P, Wu Q, Casassa G, Menzel A, Root TL, Estrella N, Seguin B, Tryjanowski P, Liu C, Rawlins S, Imeson A. Attributing physical and biological impacts to anthropogenic climate change. *Nature* 453: 353–357, 2008. doi:10.1038/nature06937.

51. Savoca MS. Chemoattraction to dimethyl sulfide links the sulfur, iron, and carbon cycles in high-latitude oceans. *Biogeochem* 138: 1–21, 2018. doi:10.1007/s10533-018-0433-2.

52. Schulte HW. Anatomy of a foetus of *Balaenoptera borealis*. *Mem Am Mus Nat Hist New Series* 1: 389–499, 2016.

53. Segre PS, Cade DE, Fish FE, Potvin J, Allen AN, Calambokidis J, Friedlaender AS, Goldbogen JA. Hydrodynamic properties of fin whale flippers predict maximum rolling performance. *J Exp Biol* 219: 3315–3320, 2016. doi:10.1242/jeb.137091.

54. Segre PS, Cade DE, Calambokidis J, Fish FE, Friedlaender AS, Potvin J, Goldbogen JA. Body flexibility enhances maneuverability in the world's largest predator. *Integr Comp Biol* 59: 48–60, 2019. doi:10.1093/icb/icy121.

55. Shadwick RE, Goldbogen JA, Potvin J, Pyenson ND, Vogl AW. Novel muscle and connective tissue design enables high extensibility and controls engulfment volume in lunge-feeding rorqual whales. *J Exp Biol* 216: 2691–2701, 2013. doi:10.1242/jeb.081752.

56. Shadwick RE, Goldbogen JA, Pyenson ND, Whale JCA. Structure and function in the lunge feeding apparatus: mechanical properties of the fin whale mandible. *Anat Rec (Hoboken)* 300: 1953–1962, 2017. doi:10.1002/ar.23647.

57. Simon M, Johnson M, Madsen PT. Keeping momentum with a mouthful of water: behavior and kinematics of humpback whale lunge feeding. *J Exp Biol* 215: 3786–3798, 2012. doi:10.1242/jeb.071092.

58. Slater GJ, Goldbogen JA, Pyenson ND. Independent evolution of baleen whale gigantism linked to Plio-Pleistocene ocean dynamics. *Proc Biol Sci* 284: 20170546, 2017. doi:10.1098/rspb.2017.0546.

59. Sokolov W. Some similarities and dissimilarities in the structure of the skin among the members of the suborders Odontoceti and Mystacoceti (Cetacea). *Nature* 185: 745–747, 1960. doi:10.1038/185745a0.

60. Stimpert AK, Wiley DN, Au WWL, Johnson MP, Arsenault R. "Megapclicks": acoustic click trains and buzzes produced during night-time foraging of humpback whales (*Megaptera novaeangliae*). *Biol Lett* 3: 467–470, 2007. doi:10.1098/rsbl.2007.0281.

61. Taheri A. On the hydrodynamic effects of humpback whale's ventral pleats. *Am J Fluid Dynamics* 8: 47–62, 2018. doi:10.5923/j.ajfd.20180802.02.

62. Taheri A. A meta-model for tubercle design of wing planforms inspired by humpback whale flippers. *Int J Aerosp Mech Engn*. 12: 315–328, 2018. doi:10.5281/zenodo.1317268.

63. Tangorra J, Phelan C, Esposito C, Lauder G. Use of biorobotic models of highly deformable fins for studying the mechanics and control of fin forces in fishes. *Integr Comp Biol* 51: 176–189, 2011. doi:10.1093/icb/icr036.

64. Vogl AW, Lillie MA, Piscitelli MA, Goldbogen JA, Pyenson ND, Shadwick RE. Stretchy nerves are an essential component of the extreme feeding mechanism of rorqual whales. *Curr Biol* 25: R360–R361, 2015. doi:10.1016/j.cub.2015.03.007.

65. Vogl W, Petersen H, Adams A, Lillie MA, Shadwick RE. The functional anatomy of nerves innervating the ventral grooved blubber of fin whales (*Balaenoptera physalus*). *Anat Rec (Hoboken)* 300: 1963–1972, 2017. doi:10.1002/ar.23649.

66. Webb PW, De Buffrénil V. Locomotion in the biology of large aquatic vertebrates. *Trans Am Fish Soc* 119: 629–641, 1990. doi:10.1577/1548-8659(1990)119<0629:LITBOL>2.3.CO;2.

67. Werth AJ. Adaptations of the cetacean hyolingual apparatus for aquatic feeding and thermoregulation. *Anat Rec (Hoboken)* 290: 546–568, 2007. doi:10.1002/ar.20538.

68. Werth AJ, Potvin J. Baleen hydrodynamics and morphology of crossflow filtration in balaenid whale suspension feeding. *PLoS One* 11: e0150106, 2016. doi:10.1371/journal.pone.0150106.

69. Werth AJ, Ito H. Sling, scoop, and squirter: anatomical features facilitating prey transport, processing, and swallowing in rorqual whales (Mammalia: Balaenopteridae). *Anat Rec (Hoboken)* 300: 2070–2086, 2017. doi:10.1002/ar.23606.

70. Werth AJ, Potvin J, Shadwick RE, Jensen MM, Cade DE, Goldbogen JA. Filtration area scaling and evolution in mysticetes: trophic niche partitioning and the curious cases of sei and pygmy right whales. *Biol J Linn Soc Lond* 125: 264–279, 2018. doi:10.1093/biolinnean/bly121.